Active filtering applied to a doubly-fed induction generator supplying nonlinear loads on isolated grid

Nicolas PATIN[1], Eric MONMASSON[2], Jean-Paul LOUIS[1]
SATIE - CNRS UMR 8029
[1]ENS de Cachan
61 av. du Président Wilson, 94235 Cachan
Emails: {patin;jplouis}@satie.ens-cachan.fr
[2]Université de Cergy-Pontoise
Rue d'Eragny, 95031 Cergy-Pontoise
Email: eric.monmasson@iupge.u-cergy.fr

Abstract

Variable speed and constant frequency (VSCF) generators are widely used in industry (e.g. embedded applications and renewable energy systems). Doubly-fed induction generators (DFIG) allow a such operation. Moreover, this kind of machines can be driven by a low power converter in comparison to the power provided to the grid. But on isolated grid, a efficient controller is needed in order to maintain quasi-sinusoidal voltages with an important amount of nonlinear load and with a small passive filter. The aim of this paper is to present a new design methodology based on the inversion of the dynamical model of the system. It also uses an original representation of the system called dynamical equivalent circuit. Thus, a hierarchical controller is designed and validated by simulation.

Keywords

Active filter, Control methods of electrical systems, Generation of electrical energy, Doubly-fed induction motor.

1 Introduction

The doubly fed induction generator (DFIG), also known as single doubly-fed machine (SDFM) [4], is widespread in the renewable energy systems as the windmills [7] and is known as a variable speed and constant frequency (VSCF) generator. We are interested here in a DFIG supplying an autonomous grid, such as an aircraft power distribution system (PDS). The full stand-alone generator we study is shown in Fig. 1. In this structure, frequencies and voltage magnitudes depend on two main parameters : speed Ω and number of pole pairs p of the DFIG. A permanent magnet synchronous machine (PMSM) maintain stand-alone operation. A PWM rectifier is used for converting three-phase ac input (from PMSM) into DC, which supplies power to an inverter connected to the rotor windings of the DFIG.

The control of this generator was already treated in [5]. In this previous case, the stator voltages are very sensitive to the current harmonics generated by a nonlinear load. This is why a filtering is necessary to maintain a low voltage disturbance [6]. The innovating aspect of the presented work concerns the design of a controller carrying out an active filtering for an autonomous grid through the DFIG, as it is already done with synchronous machines [1], [2] but also with a DFIG connected to the utility grid [3]. Thus, the size and the weight of the passive filter components can be minimized: these two quantities are particularly significant criteria in embedded systems like aircraft applications. For this study, we use a vector dynamical equivalent circuit representation of the machine

1

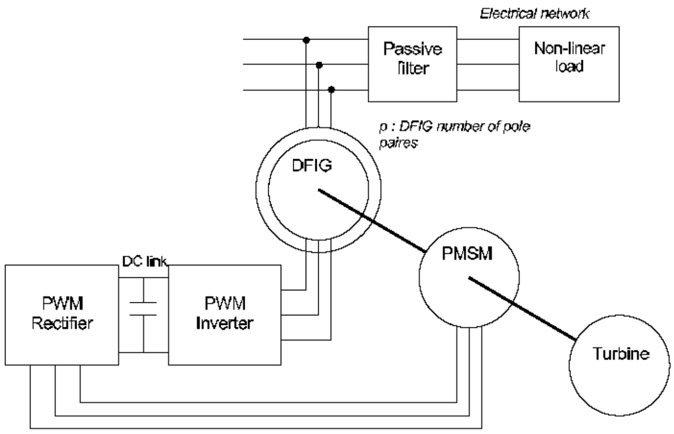

Figure 1: Full stand-alone doubly-fed induction generator

and its load. These elements are presented in Section II. Then, we detail the successive levels of our controller: initially, regulation of the rotor currents, then the control of the stator voltages. In both cases, we use the dynamic equations of the DFIG to highlight the suitable state feedbacks that allow decoupling of dq axes. This controller is tested in simulation to validate the two focused objectives: obtaining a constant frequency and magnitude of the voltage grid (IV.A-for a linear load and IV.B-for a nonlinear load). The latter objective implies that the DFIG works as an active filter. The results for a nonlinear load are compared with that obtained with a classical control strategy without active filtering. As exposed in section IV, active filtering has a significant effect on the voltages and currents imposed in the rotor windings of the DFIG. Finally, the influence of the value of the passive filter capacitors is studied.

2 System modelling

2.1 Dynamical equivalent circuits

We propose in this section two vector dynamical equivalent circuits of the DFIG (Fig. 2) and the load (Fig. 3). The behaviour of the DFIG can be described by the following equations in an unspecified dq frame

$$\left\{ \begin{array}{l} \mathbf{v}_{dq} = R_s \mathbf{i}_{dq} + \frac{d\psi_{dq}}{dt} + \dot{\xi}_s \cdot \mathrm{J}_2 \cdot \psi_{dq} \\ \mathbf{v}_{DQ} = R_r \mathbf{i}_{DQ} + \frac{d\psi_{DQ}}{dt} + \dot{\xi}_r \cdot \mathrm{J}_2 \cdot \psi_{DQ} \end{array} \right. \tag{1}$$

where fluxes are

$$\left\{ \begin{array}{l} \psi_{dq} = L_{cs} \mathbf{i}_{dq} + M \mathbf{i}_{dq} \\ \psi_{DQ} = M \mathbf{i}_{dq} + L_{cr} \mathbf{i}_{DQ} \end{array} \right. \tag{2}$$

The relationship between the stator and rotor frame angles ξ_s, ξ_r and the mechanical angular position of the rotor θ is

$$\xi_s = \xi_r + p\theta \tag{3}$$

All the parameters introduced in (1,2,3) are defined as follows

- R_s and R_r are stator and rotor resistances
- L_{cs} and L_{cr} are stator and rotor inductances
- M is the mutual inductance between stator and rotor windings

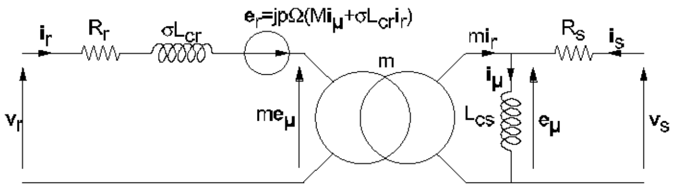

Figure 2: Equivalent circuit of the DFIG

- p is the number of pole pairs of the DFIG

Then, a dynamical equivalent circuit of the DFIG can be derived from these equations (see Fig. 2). The proposed circuit has been established in the fixed stator frame and leakage inductance is located to the rotor side (with $\sigma = 1 - \frac{M^2}{L_{cs}L_{cr}}$). The back e.m.f. $\underline{e}_r$ (which can be seen at the rotor side) is defined as follows

$$\underline{e}_r = jp\Omega\left(M\underline{i}_\mu + \sigma L_{cr}\underline{i}_r\right) \tag{4}$$

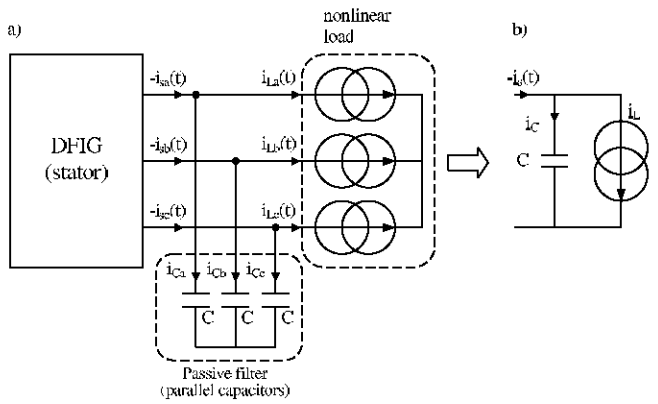

Figure 3: Three-phase nonlinear load with parallel capacitors (a) and its dynamical equivalent circuit (b)

A dynamical equivalent circuit of the load with parallel capacitors is proposed in Fig. 3. Notice that this equivalent circuit is also established in the DFIG stator frame. Thus, it is possible to connect directly these two dynamical equivalent circuits. However, it is useful to transform this global model in order to work with constant quantities in our controller (using PI regulators). The transformation needed is a simple rotation which is translated in the dynamical equivalent circuit by the effects presented in Fig. 4.

Thus, we obtain a global dynamical equivalent circuit in a reference frame linked to the grid voltages as shown in Fig. 5.

In this equivalent circuit, three new sources are introduced :

$$\begin{cases} \underline{e}'_r = j\left(\omega_g \sigma L_{cr}\underline{i}_r - p\Omega\left(M\underline{i}_\mu + \sigma L_{cr}\underline{i}_r\right)\right) \\ \underline{e}_{\mu 0} = jL_{cs}\omega_g\underline{i}_\mu \\ \underline{i}_{C0} = jC\omega_g\underline{v}_s \end{cases} \tag{5}$$

where ω_g is the grid angular frequency.

 ISBN : 90-75815-08-5

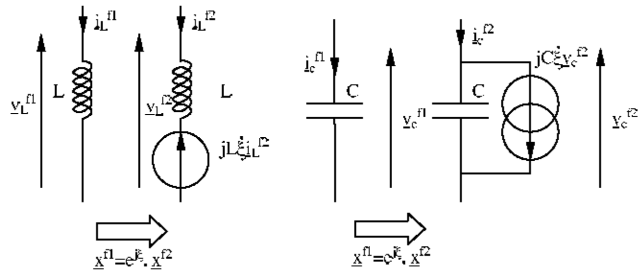

Figure 4: Transformation by rotation of reactive components (from f1 reference frame to f2 reference frame)

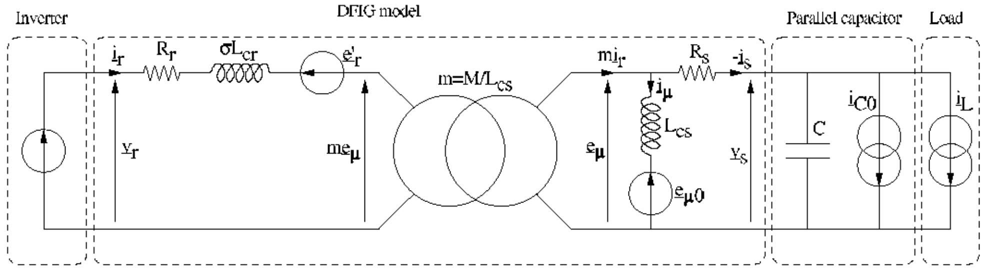

Figure 5: Global dynamical equivalent circuit in a grid synchronous frame

2.2 State-space model

A global state-space model can be easily derived from the dynamical equivalent circuit presented in Fig. 5. Therefore, we define a complex state vector $\mathbf{x}$, a control input u, a disturbance input ϖ and an output y

$$\left\{\begin{array}{l} \mathbf{x} = \left(\underline{i}_r, \underline{i}_\mu, \underline{v}_s\right)^t \\ u = \underline{v}_r \\ \varpi = \underline{i}_L \\ y = \underline{v}_s \end{array}\right. \tag{6}$$

and the model which is established below depends on the mechanical speed Ω[1]

$$\left\{\begin{array}{l} \dot{\mathbf{x}} = K(\Omega, \omega_g).\mathbf{x} + L_1 u + L_2 \varpi \\ y = M.\mathbf{x} \end{array}\right. \tag{7}$$

where the matrices $K(\Omega, \omega_g)$, L_1, L_2 and M are defined as follows

$$K(\Omega,\omega_g) = \begin{pmatrix} k_{11}(\Omega,\omega_g) & k_{12}(\Omega) & k_{13} \\ k_{21} & k_{22}(\omega_g) & k_{23} \\ k_{31} & k_{32} & k_{33}(\omega_g) \end{pmatrix} ; \; L_1 = \begin{pmatrix} \frac{1}{\sigma L_{cr}} \\ 0 \\ 0 \end{pmatrix} ; \; L_2 = \begin{pmatrix} 0 \\ 0 \\ -\frac{1}{C} \end{pmatrix}$$

$$M = \begin{pmatrix} 0 & 0 & 1 \end{pmatrix}$$

with

$$\left\{\begin{array}{l} k_{11}(\Omega,\omega_g) = -\frac{R_r + m^2 R_s + j(p\Omega - \omega_g)}{\sigma L_{cr}} \\ k_{21}(\Omega) = \frac{m R_s}{L_{cs}} \\ k_{31} = \frac{m}{C} \end{array}\right. ; \; \left\{\begin{array}{l} k_{12}(\Omega) = \frac{m R_s + jpM\Omega}{\sigma L_{cr}} \\ k_{22}(\omega_g) = -\frac{R_s}{L_{cs}} - j\omega_g \\ k_{32} = -\frac{1}{C} \end{array}\right. ; \; \left\{\begin{array}{l} k_{13} = -\frac{m}{\sigma L_{cr}} \\ k_{23} = \frac{1}{L_{cs}} \\ k_{33}(\omega_g) = -jC\omega_g \end{array}\right.$$

[1] In our application, we suppose that the power of the mechanical drive is very large with regard to electrical power of the generator. Thus, the speed Ω can be seen like a DFIG parameter and not like a state variable.

 ISBN : 90-75815-08-5

3 DFIG control

3.1 Principle

We suggest the use of a hierarchical controller, with first of all an inner regulation loop of the rotor current $\underline{i}_r$. Then, an external loop allows us to control the stator voltages of the DFIG (*i.e.* of the grid voltages). Then, a stator voltage loop (outer loop) is designed to keep constant the magnitude of the grid voltages. Thus, the stator voltages are controlled via the rotor current reference, noted $\underline{i}_r^{\mathrm{ref}}$ which is supposed equal to $\underline{i}_r$ as long as the inner loop is fast enough to follow the reference.

3.2 Inner rotor current loop

In order to impose the dynamics of the rotor current $\underline{i}_r$, the control of the rotor impedance voltage v_{RL} is required. Thus, it is possible to drive the rotor voltage according to

$$\underline{v}_r = v_{RL} + \widehat{\underline{e}}_r' + m\widehat{\underline{e}}_\mu \tag{8}$$

where $\widehat{\underline{e}}_r'$ and $\widehat{\underline{e}}_\mu$ are the estimated value of $\underline{e}_r'$ and $\underline{e}_\mu$ respectively, defined as follows

$$\begin{cases} \widehat{\underline{e}}_r' = j\left(\omega_g \sigma L_{cr} \underline{i}_r^{\mathrm{meas}} - p\Omega\left(M\widehat{\underline{i}}_\mu + \sigma L_{cr}\underline{i}_r^{\mathrm{meas}}\right)\right) \\ \widehat{\underline{e}}_\mu = \underline{v}_s^{\mathrm{meas}} - R_s \underline{i}_s^{\mathrm{meas}} \end{cases} \tag{9}$$

where $\underline{i}_\mu$ is also estimated. While $\underline{i}_s$ and $\underline{i}_r$ are measured, a very simple estimator is proposed

$$\widehat{\underline{i}}_\mu = m\underline{i}_r^{\mathrm{meas}} + \underline{i}_s^{\mathrm{meas}} \tag{10}$$

Notice that the meas superscript means that the quantity is measured.

Then, v_{RL} is the output of a PI controller dedicated to the regulation of $\underline{i}_r$ as we can see in Fig. 6.

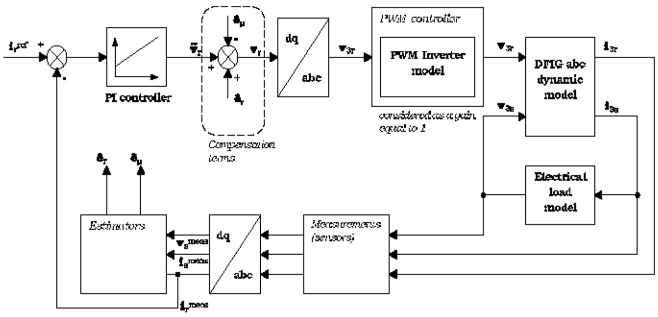

Figure 6: Inner rotor current loop

3.3 Controlled DFIG model

Now, considering that the rotor current is controlled, the dynamical equivalent circuit presented in Fig. 5 is replaced by the one in Fig. 7.

In this figure, we are able to distinguish two state variables linked two the reactive components L_{cs} and C. Notice that it is not necessary to control the magnetizing current because this state variable is strongly coupled to the stator voltage (stator resistance neglected : $\underline{v}_s = \underline{e}_\mu$).

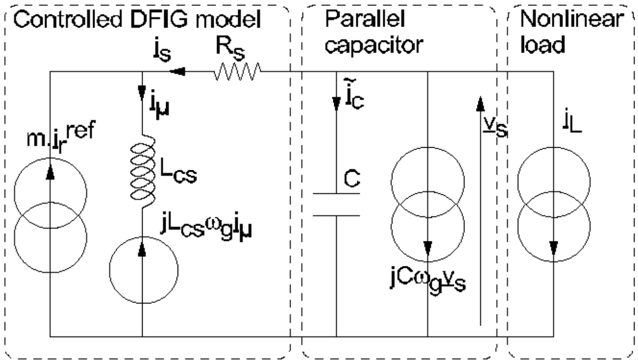

Figure 7: Controlled DFIG model

3.4 Stator voltage control

With this help of the dynamical equivalent circuit presented in Fig. 7, a stator voltage loop is designed. In the same way that for the rotor current loop, the dynamics of the stator voltage is controlled by the capacitor current $\widetilde{\underline{i}}_C$. Thus, it is necessary to generate a rotor current reference equal to

$$\underline{i}_r^{\text{ref}} = \frac{1}{m}\left(\widehat{\underline{i}}_\mu + \widetilde{\underline{i}}_C + \widehat{\underline{i}}_{C0} + \underline{i}_L^{\text{meas}}\right) \tag{11}$$

where

$$\begin{cases} \widehat{\underline{i}}_\mu = \frac{\underline{v}_s^{\text{meas}}}{jL_{cs}\omega_g} \\ \widehat{\underline{i}}_{C0} = jC\omega_g \underline{v}_s^{\text{meas}} \end{cases} \tag{12}$$

Notice that the magnetizing current estimator is quite approximative but, as we can see in the following section, the simulation results are nevertheless satisfying. Moreover, it is very simple to realize and it is a great advantage for real-time implementation. Then, the $\widetilde{\underline{i}}_C$ term is the output of the grid voltage PI controller as we can see in Fig. 8. Notice that, if all the compensation terms in (11) are given without error, a simple proportional corrector is enough. In practical cases, a PI regulator allows a *more robust control* of the grid voltage.

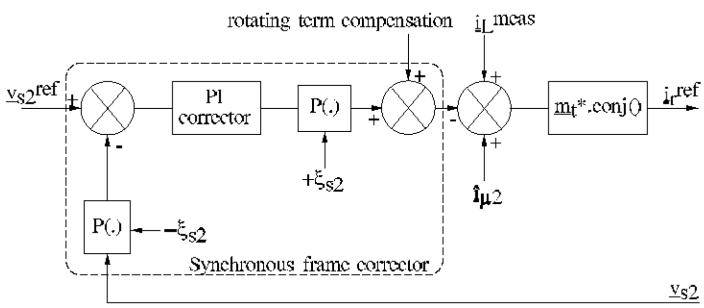

Figure 8: Stator voltage controller

The controller tuning is presented in the Fig. 9.

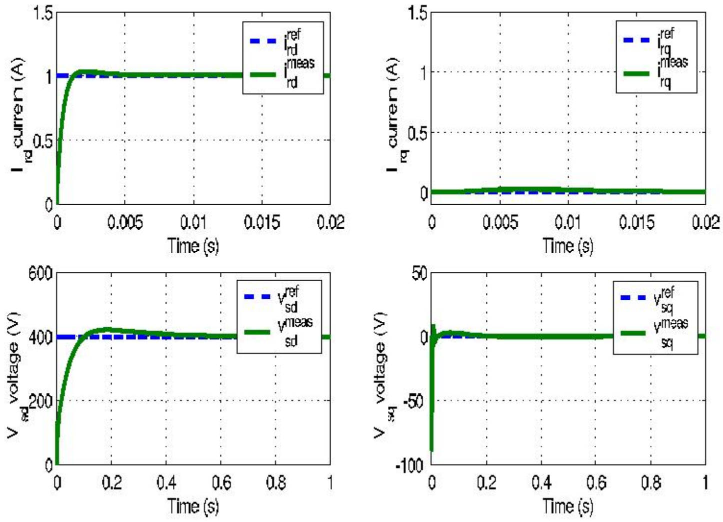

Figure 9: Controller tuning

4 Simulation results

4.1 Simulation parameters

In the following simulations, a 4kW – 50Hz doubly-fed induction machine is used in order to create a 230V – 50Hz autonomous grid. All the parameters are defined in TABLE 1.

Table 1: Simulation parameters

DFIMs parameters	Values
Numbers of pole pairs	2
Rated power of the two DFIMS	4kW
Stator resistances	1.154Ω
Rotor resistances	2.48Ω
Stator cyclic inductances	2.017H
Rotor cyclic inductances	2.015H
Stator/Rotor mutual inductances	1.986H
Coefficient of dispersion	0.031
Linear load parameters	
Resistance R	40Ω
Inductance L	1mH
Filtering capacitor C	1μF

4.2 DFIG supplying a linear load

The checking of the correct working of our controller is carried out with a linear load through two tests ;

- a test at variable speed with a fixed load (Fig. 10): from -50% to +33% of the synchronous speed.
- a test at constant speed with a variable load (impact of load - Fig. 11): from 50% to 100% of the rated load.

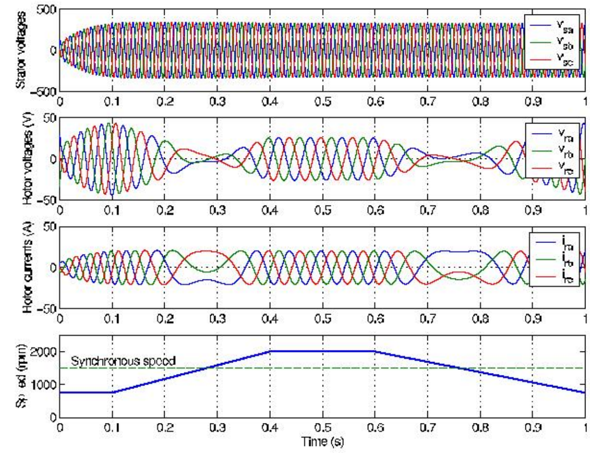

Figure 10: Variable speed and constant frequency operation

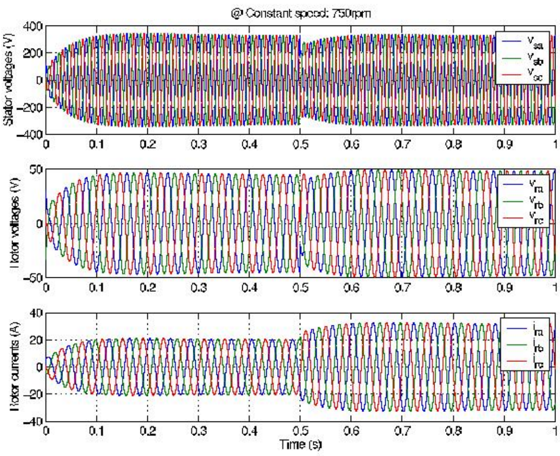

Figure 11: DFIG behaviour with a variation of load

Notice that the relationship between stator, rotor and mechanical power is also verified with a variable speed simulation. With a constant linear load, the voltage controlled DFIG provides constant power to the grid. Thus, the rotor power is proportional to the slip ratio $s = \frac{\omega_g - p\Omega}{\omega_g}$ as we can see in Fig. 12.

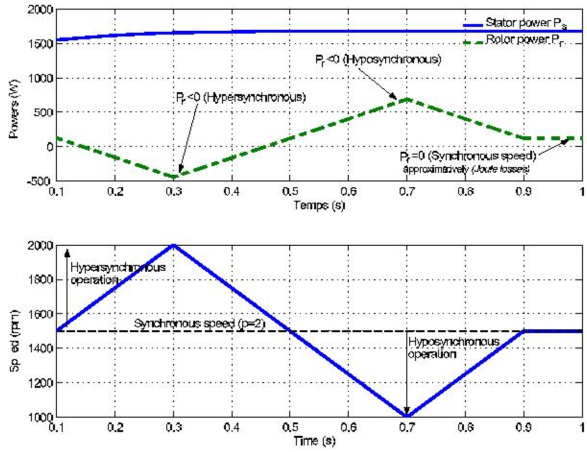

Figure 12: Powers in the DFIG

4.3 DFIG supplying a nonlinear load

We can see in Fig. 13 that due to the fact of active filtering, grid voltages are quasi-sinusoidal despite the significant amount of nonlinear load (100% of the rated load).

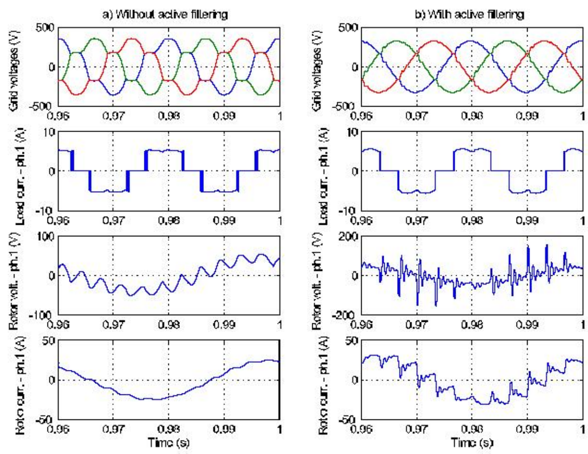

Figure 13: Active filtering operation (a - without and b - with active filtering)

However, the active filtering requires high rotor voltages which can exceed the maximum value provided by the inverter or become excessive for electrical insulators. This negative impact can be compensated by increasing the values of the passive filter capacitors. Several simulations have been computed with the same load but with different capacitors values: the maximum rotor currents and voltages are shown versus the capacitors value (Fig. 14).

The problem leads to a trade-off between the size of capacitors and the DC link voltage required by the active filtering (which have large consequences on all the elements of the generator presented in Fig. 1).

 ISBN : 90-75815-08-5

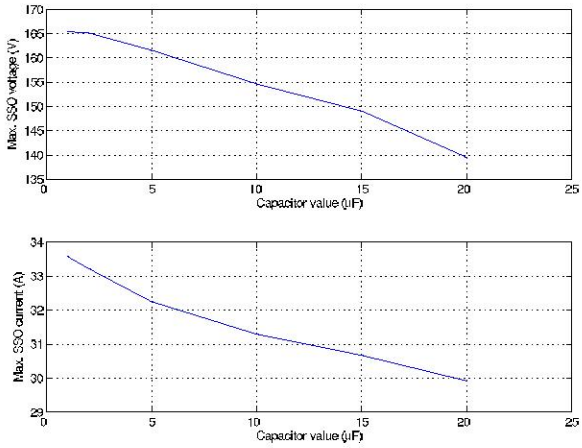

Figure 14: Capacitor choice consequences

5 Conclusions

In this paper, a DFIG model and a new VSCF controller have been proposed for an autonomous grid. This controller allows supplying linear and nonlinear loads by sinusoidal voltages with only small parallel capacitors. Obtaining an efficient active filtering depends on several parameters such as the rotor impedance of the DFIG and the PWM frequency which can reduce the rotor current bandwidth. But the efficiency of this method is proved if the system parameters are compatible with the load dynamics. Moreover, we are able with the proposed control strategy to select the harmonics we want to compensate (e.g. 5^{th}, 7^{th}, 11^{th}).

References

[1] M. T. Abolhassani, H. A. Toliyat, P. Enjeti, *Harmonic compensation using advanced electric machines*, in Proc. IEEE-IECON'01 Conf., pp. 1388-1393, Denver, USA, Nov. 2001.

[2] M. T. Abolhassani, H. A. Toliyat, P. Enjeti, *An electromechanical active harmonic filter*, in Proc. IEEE-IEMDC'01 Conf., pp. 349-355, Cambridge, USA, June 2001.

[3] M. T. Abolhassani, H. A. Toliyat, P. Enjeti, *Stator flux oriented control of an integrated alternator/Active filter for wind power applications*, in Proc. IEEE-IEMDC'03 Conf., pp. 461-467, Madison, USA, June 2003.

[4] B. Hopfensperger, *Doubly-fed a.c. machines : classification and comparison*, in Proc. EPE'01 Conf., CD-ROM, Graz, Austria, Aug. 2001.

[5] F. Khatounian, E. Monmasson, F. Berthereau, E. Delaleau, J.-P. Louis, *Control of a Doubly-Fed Induction Generator for Aircraft Application*, in Proc. IEEE-IECON'03 Conf., pp. 2711-2716, Roanoke, USA, Nov. 2003.

[6] F. Khatounian, E. Monmasson, F. Berthereau, J.-P. Louis, *Design of an Output LC Filter for a Doubly-Fed Induction Generator for Aircraft Application*, in Proc. IEEE-ISIE'04 Conf., Ajaccio, France, May 2004.

[7] S. Muller, R. W. De Doncker, *Doubly-fed induction generator systems for wind turbines*, IEEE Industry Applications Magazine, Vol. 8, No. 3, pp. 26-33, May-June 2002.

 ISBN : 90-75815-08-5